Bulletin de la Société Royale des Sciences de Liège, Vol. 80, 2011, p. 673 - 677

The X-ray emission of the colliding wind binary V444 Cyg

Thomas Fauchez[1], Michaël De Becker[1,2] & Yaël Nazé[1]

[1] Department of Astrophysics, Geophysics and Oceanography, University of Liège, Belgium
[2] Observatoire de Haute-Provence, Saint-Michel l'Observatoire, France

Abstract: This paper presents the analysis of six *XMM-Newton* observations of the colliding wind system V444 Cyg. Unlike what one might have expected at first, it appears that the O star wind most probably dominates the WN wind: the bow shock is wide open, with the hard X-ray emission arising close to the WN star. An important radiative braking could partly explain this situation but revising the wind parameters may also prove necessary. Furthermore, we have probably observed for the first time an occultation of the colliding wind zone by the binary components.

1 Scientific context

V444 Cyg is a close colliding wind binary system made up of an O6 star and a WN5 star. It is a double eclipse system with a period of ∼4.2 days. The physical parameters are summarized in Table 1. Using these parameters, we have calculated the pre-shock velocities of both winds, assuming that the winds obey the following velocity law: $v_j(r) = v_{\infty,j}(1-\frac{R_j}{r_j})^{\beta_j}$, with j indicating the number of the star (1 for the WN and 2 for the O-star), $v_{\infty,j}$ being the terminal wind speed of the jth star, R_j the stellar radius of the jth star, r_j the radial distance to star j and β being equal to 1 for both stars (Hamann & Schwarz 1992). We obtained a pre-shock velocity value of 2204 km s^{-1} for the WN wind and 441 km s^{-1} for the O star wind. These velocities result in post-shock temperatures of about 9 keV. Note that this value is an upper limit since the Rankine-Hugoniot equations do not take into account the phenomenon of radiative braking.

2 Observations

For our study of the V444 Cyg system, six exposures taken by *XMM-Newton* in 2004 (Obs. ID 020624) were available. These observations covered half an orbit (i.e. they were taken at phases 0.02, 0.12, 0.28, 0.39, 0.49, and 0.51) with a nominal exposure time by observation of 10 ks. Note that phase 0 corresponds to the phase where the WR is in front of the O-star.

	WR star	O star	Ref
P_0 [days]	4.212450 ± 0.000048		1
T_0 [julian days]	2438636.867		2
Incl. angle [deg]	78		3
Distance[kpc]	1.7		4
$f(m)[M_\odot]$	12.9 ± 0.3	1.1 ± 0.1	5
$M[M_\odot]$	12.4 ± 0.5	28.4 ± 0.6	5
$\dot{M}[M_\odot\ yr^{-1}]$	4.6×10^{-6}	5.8×10^{-7}	5
$R[R_\odot]$	2.9	10	6
$a[R_\odot]$	26.2 ± 0.3	11.5 ± 0.3	5
$\gamma[km\ s^{-1}]$	45 ± 1	-26 ± 2	5
$K[km\ s^{-1}]$	309 ± 2	136 ± 3	5
$\omega[deg]$	268.6 ± 0.4	88.0 ± 1.0	5
$v_\infty[10^3 km\ s^{-1}]$	2.5	1.7	7

Table 1: Physical parameters of V444 Cyg. References are (1) Pelt (1992); (2) Underhill et al. (1990); (3) Cherepashchuk, Eaton & Khaliullin (1984); (4) Forbes (1981); (5) Hirv et al. (2006); (6) Corcoran et al. (1996); (7) Stevens et al. (1992)

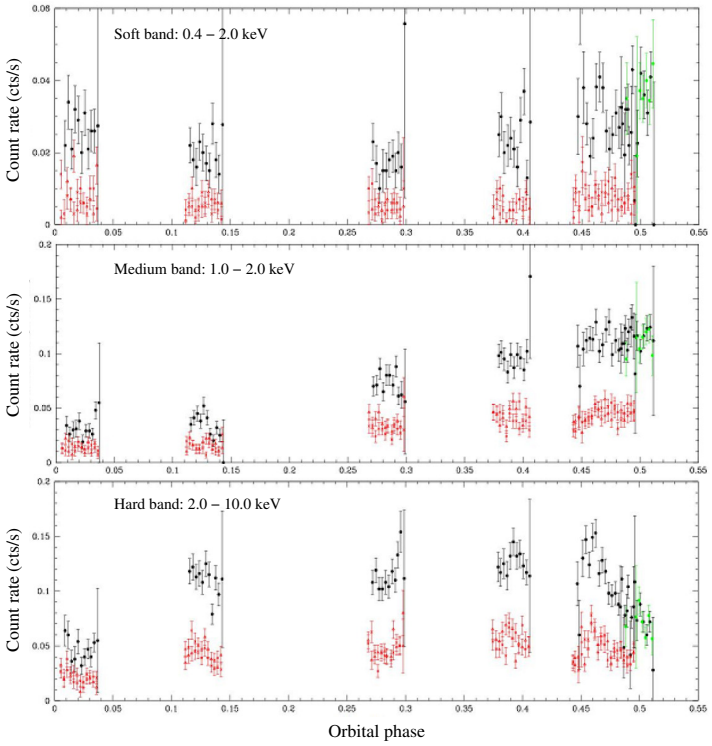

Figure 1: Variations of the count rates in three energy bands. The black and green circles correspond to EPIC-pn data, while crosses and red triangles indicate EPIC-MOS data.

3 Light curve analysis

Figure 1 shows the evolution of the EPIC count rates with orbital phase for three different energy bands. In the soft band (0.4-2 keV), the count rate is always significantly low because the absorption is particularly strong in this system, thus it shows only weak variations (not statistically significant) over the orbit. The medium band (1-2 keV) count rate decreases when

the system is seen through the opaque wind of the WN. However, this flux decrease occurs only over a short phase interval, implying that the O-star wind dominates that of the WN and that the bow shock is probably wide open. This can probably be explained by the phenomenon of radiative braking. Indeed, simulations of Owocki & Gayley (1995) showed that, provided radiative braking is strong enough, the bow shock could be widely open. By contrast, the hard band (2-10 keV) count rate remains stable over the orbit, except at the phases corresponding to the optical eclipses. Indeed, a large decrease of the count rate is observed between the phases $\phi = 0.00$ and $\phi = 0.04$ and between the phases $\phi = 0.45$ and $\phi = 0.50$. This could be easily explained if the stars occult the zone emitting the hard X-rays at these phases. In this case, a sketch of the system (Fig. 2) suggests that the allowed position of the hot plasma (green hatched area) is close to the WN star, in other words far from the theoretical stagnation point (black dot). This difference is probably due to radiative braking, but not only, as simulations by Owocki & Gayley (1995) do not result in a colliding-wind zone wrapped around the WN star. Therefore, a revision of the system's physical parameters (mass-loss rate, wind velocity) is probably needed.

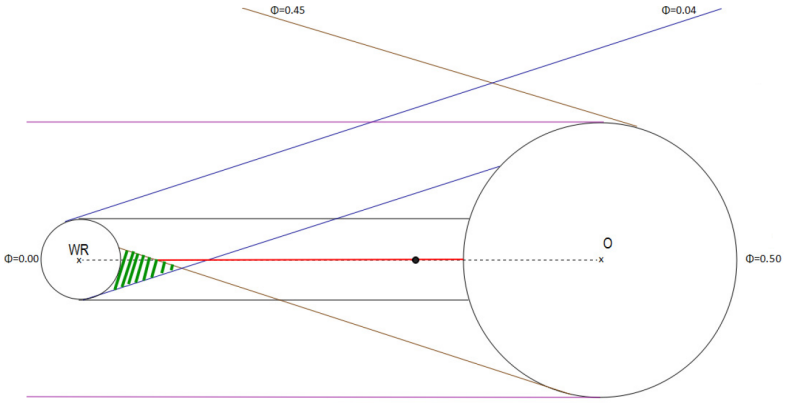

Figure 2: Sketch to scale of the V444 Cyg system (assuming an inclination of 90°). The dotted line joins the stars' centers; the black dot on this line represents the theoritical position of the stagnation point when solely considering ram-pressure balance. The grey and blue parallel lines bound the zone eclipsed by the WN at phases $\phi = 0.00$ and $\phi = 0.04$, respectively; the purple and brown parallel lines bound similar zones, but eclipsed by the O-star at phases $\phi = 0.45$ and $\phi = 0.50$, respectively. The green hatched area corresponds to the area eclipsed during both phase intervals $0 < \phi < 0.04$ and $0.45 < \phi < 0.5$. If the occultation hypothesis is correct, then a significant fraction of the hot plasma due to the colliding winds should be located there.

4 Spectral analysis

The spectral fitting was done using a progressive approach, i.e. we freed one physical parameter at a time. This careful approach allowed us to obtain physically realistic spectral parameters. First of all, we used a very simple model with one global absorption component and two optically-thin thermal plasma emission components, i.e. $wabs \times (apec + apec)$. Next, we associated an individual absorption component to each emission component and used a global absorption component fixed to the interstellar value of $0.32 \times 10^{22}\,\mathrm{cm}^{-2}$ (Oskinova 2005), i.e. the model has the form $wabs_{ISM} \times (wabs \times apec + wabs \times apec)$. In this case, whatever the orbital phase, we obtained temperatures of the order of ∼0.6 keV and ∼2.0 keV for the thermal

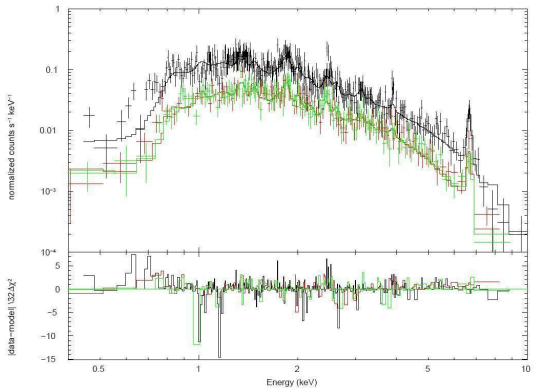

Observation	n_{H1} $[10^{22} cm^{-2}]$	norm 1 $[10^{-3} cm^{-5}]$	n_{H2} $[10^{22} cm^{-2}]$	norm 2 $[10^{-3} cm^{-5}]$	reduced χ^2 dof	absorbed flux unabsorbed flux $[erg\ cm^{-2}\ s^{-1}]$
Obs 1	$0.67^{0.77}_{0.58}$	$0.52^{0.63}_{0.43}$	$7.11^{7.67}_{6.60}$	$3.74^{4.01}_{3.48}$	1.03 306	1.15×10^{-12} 1.26×10^{-12}
Obs 2	$0.49^{0.57}_{0.43}$	$0.45^{0.53}_{0.38}$	$11.81^{13.90}_{9.99}$	$2.41^{2.83}_{2.03}$	1.20 264	0.62×10^{-12} 0.76×10^{-12}
Obs 3	$0.77^{0.92}_{0.58}$	$1.47^{2.12}_{0.83}$	$2.10^{3.17}_{1.31}$	$1.14^{1.35}_{0.95}$	0.96 141	0.87×10^{-12} $1,10 \times 10^{-12}$
Obs 4	$1.12^{1.22}_{1.02}$	$2.07^{2.51}_{1.68}$	$3.51^{3.98}_{3.09}$	$2.69^{2.89}_{2.51}$	1.05 447	1.36×10^{-12} 1.54×10^{-12}
Obs 5	$1.09^{1.23}_{0.94}$	$1.45^{1.90}_{1.05}$	$3.19^{3.68}_{2.77}$	$2.23^{2.40}_{2.08}$	1.08 346	1.14×10^{-12} 1.28×10^{-12}
Obs 6	$0.99^{1.06}_{0.91}$	$2.04^{2.39}_{1.70}$	$2.69^{3.04}_{2.38}$	$2.04^{2.24}_{1.87}$	1.01 617	1.24×10^{-12} 1.46×10^{-12}

Figure 3: *Left*: Best-fit model superimposed on the observed spectra (MOS 1 & 2 data shown in green and red, respectively, pn data in black) of the 6th observation (i.e. ϕ=0.51). *Right*: Best-fit spectral parameters for the final model. n_{H1} and n_{H2} represent the column densities in front of the first and second emission component, respectively, and $norm_1$ and $norm_2$ represent the normalization parameters of the first and second emission component. The plasma temperatures were fixed to the values of 0.59 and 2.01 keV, respectively, for the two emission components. The nitrogen abundance was fixed to 101.3 (best-fit value for the 6th observation), while those of carbon and oxygen were fixed to 0. Other abundances were frozen to solar values.

components. Since these temperatures did not seem to vary with phase, we froze them and then successively allowed the abundances of nitrogen, carbon, oxygen and iron of the emission components to vary. The abundances of some elements deviate significantly from the solar values: N presents a significant overabundance, while abundances of C and O are compatible with a null value. We did not notice any significant deviation from the solar value for the iron abundance. Our best-fit parameters were obtained when we fixed the plasma temperatures and abundances to the values for the highest quality observation (ϕ=0.51), allowing only local absorbing columns and normalization parameters to vary from one observation to the other. This approach was necessary to achieve a consistent modelling of the EPIC spectrum of V444 Cyg as a function of the orbital phase. The results are shown in Fig. 3.

The absorption and normalization factors of the cooler thermal component appear constant over the orbit. Moreover, the column density is quite small (with regard to the high density of the WN wind). This can be explained if the soft emission is intrinsic to the stellar winds and takes place far from the two stars. The normalization factor of the hotter emission component varies only slightly but its absorption varies strongly with orbital phase. It should indeed reach its maximum when the system is seen through the WN wind. This situation occurs between the phases $\phi = 0.00$ and $\phi = 0.12$. It is a surprisingly short phase interval, implying that the O-star wind clearly dominates the WN wind. Therefore, the bow shock should be wide open and may even wrap around the WN star.

5 Comparison with previous studies

V444 Cyg has been a target for several X-ray observatories: EINSTEIN (Moffat et al. 1982; Pollock 1987), ROSAT (Corcoran et al. 1996), ASCA (Maeda, Koyama & Yokogawa 1999). These campaigns already pointed out the presence of a probable contribution of the X-rays coming from colliding winds. The analysis of ASCA data led to a global description of the

X-ray spectrum in good agreement with ours: the spectrum is of thermal origin, with typical temperatures of the order of 0.6 and 2.0 keV. Maeda et al. (1999) also detected some variations in the X-ray spectrum as a function of the orbital phase (in particular in the hard part), but did not interpret them in terms of a potential occultation of the colliding-wind region.

More recently, the same *XMM-Newton* data set as presented here was analyzed by Bhatt et al. (2010). These authors obtained comparable lightcurves but do not interpret them. Furthermore, their spectral analysis was made in a very different manner: a complex model, with many free parameters, was used right away. This resulted in erratic results, sometimes unphysical, without satisfactory coherence between the results obtained at different orbital phases.

6 Concluding remarks

Our spectral and lightcurve analyses of the *XMM* data of V444 Cyg provided unexpected results. First, the evolution of the medium-band count rate and of the fitted absorption shows that the observed flux decreases when the system is seen through the WN wind. As this occurs over a short phase interval, this implies that the bow shock is widely open, maybe even folded around the WN star. In addition, the evolution of the flux observed in the hard band strongly suggests the occultation of a significant fraction of the hard X-ray emitting region, at orbital phases close to conjunctions. If confirmed, this result would constitute the first detection of occultations by stars of the hot plasma produced by a wind-wind collision. It must be noted that, in this framework, the hard X-ray emission should arise close to the WN star. These two results may be explained if one takes into account a strong radiative braking, perhaps combined to a revision of the wind parameters.

Acknowledgements

The authors acknowledge support from the XMM+INTEGRAL PRODEX contracts (Belspo) and the FRS/FNRS (Belgium). Our thanks go also to the referee for useful comments that significantly improved the present manuscript.

References

Bhatt, H., Pandey, J.C., Kumar, B., Singh, K.P. & Sagar, R. 2010, MNRAS 402, 1767
Cherepashchuk, A., Eaton, J., & Khaliullin, K. 1984, ApJ 281, 774
Corcoran, M.F., Stevens, I.R., Pollock, A.M.T., Swank, J.H., Shore, S.N. & Rawley, G.J. 1996, ApJ 464, 434
Forbes, D. 1981, PASP 93, 441
Hamann, W.-R., & Schwarz, E. 1992, A&A 261, 523
Hirv, A., Annuk, K., Eenmäe, T., Liimets, T., Pelt, J., Puss, A. & Tempel, M. 2006, Baltic Astronomy 15, 405
Maeda, Y., Koyama, K. & Yokogawa, J. 1999, ApJ, 510, 967
Moffat, A.F.J, Firmani, F., McLean, I.S., & Seggewiss, W. 1982, in *Wolf-Rayet Stars: Observations, Physics, Evolution*, IAU Symp 99, eds. de Loore, C.W.H. & Willis A.J., 577
Oskinova, L. 2005, MNRAS 361, 679
Owocki, S.P., & Gayley, K.G. 1995, ApJ 145, 148
Pollock, A.M.T. 1987, ApJ, 320, 283
Pelt, J. 1992, in *Irregular Spaced Data Analaysis - User Manual*, Helsinki University Press
Stevens, I.R., Blondin, J.M., & Pollock, A.M.T. 1992, ApJ 265, 287
Underhill, A.B., Grieve, G.R., & Louth, H. 1990, PASP 102, 749